Distance Measurement Using a Single Camera with a Rotating Mirror

Hyongsuk Kim, Chun-Shin Lin, Jaehong Song, and Heesung Chae

Abstract: A new distance measurement method with the use of a single camera and a rotating mirror is presented. A camera in front of a rotating mirror acquires a sequence of reflected images, from which distance information is extracted. The distance measurement is based on the idea that the corresponding pixel of an object point at a longer distance moves at a higher speed in a sequence of images in this type of system setting. Distance measurement based on such pixel movement is investigated. Like many other image-based techniques, this presented technique requires matching corresponding points in two images. To alleviate such difficulty, two kinds of techniques of image tracking through the sequence of images and the utilization of multiple sets of image frames are described. Precision improvement is possible and is one attractive merit. The presented approach with a rotating mirror is especially suitable for such multiple measurements. The imprecision caused by the physical limit could be improved through making several measurements and taking an average. In this paper, mathematics necessary for implementing the technique is derived and presented. Also, the error sensitivities of related parameters are analyzed. Experimental results using the real camera-mirror setup are reported.

Keywords: Distance measurement, matching, monocular vision, precision improvement.

1. INTRODUCTION

Distance measurement is one desired capability for an intelligent robot to understand its working environment. Among existing distance-measurement techniques, one category imitates the human vision and evaluates the distance using the spatial disparity of an object point in two images. The measurement system typically consists of a pair of cameras. The distance is computed using the disparity of two corresponding pixels with the triangulation [1-3,10]. The two cameras must be carefully aligned and well-calibrated to minimize the measurement inaccuracy. If the characteristics of two cameras are not identical due to a difference in fabrication, an impact or aging, a significant measurement error could be hard to avoid [11,12]. Some researchers elaborated on the monocular vision [4-8,16] for possibly overcoming the shortcomings of the stereo-vision measurement system. With two images taken at two different positions by a single camera, the distance information can be computed in the similar way as that with the stereo-vision. The robotic eye-in-hand system, which has a camera moved by a robot arm [5-8,16], is an example. Since the movement of the camera on the robot arm is omni-directional, finding the matching points on images could be computationally costly. Hazard on the camera is more likely due to the frequent movement and impact. Physically moving the robot arm also causes a significant amount of delay on distance measurement. Other researchers suggested a measurement system with a camera and two fixed plane mirrors [9,14,15]. Stereo images reflected from the two mirrors are acquired by the single camera. With two fixed mirrors, the field of view is reduced and becomes narrower. Convex mirrors had been suggested to replace plane mirrors [13,14] to increase the viewable and measurable area. However, image distortion caused by the convex mirrors becomes a major problem.

In this study, a system that is composed of a single camera and a rotating mirror is investigated. The camera acquires a sequence of images from the rotating mirror. The distance is measured utilizing the

Manuscript received October 21, 2004; revised June 23, 2005; accepted October 7, 2005. Recommended by Editorial Board member Wankyun Chung under the direction of Editor Keum-Shik Hong. This work was supported by Electronics and Telecommunications Research Institute (ETRI) and Ministry of Information and Communication (MIC), Korea.

Hyongsuk Kim is with the Center for Advanced Image and Information Technology, Division of Electronics and Information Engineering, Chonbuk National University, 664-14 1ga Duckjin-Dong Duckjin-Gu Jeonju, Jeonbuk 561-756, Korea (e-mail: hskim@moak.chonbuk.ac.kr).

Chun-Shin Lin is with the Department of Electrical and Computer Engineering, University of Missouri, Columbia, MO, USA (e-mail: LinC@missouri.edu).

Jaehong Song is with the Blue Code Technology Co. Ltd. Daejeon, Korea (e-mail: jhsong@syswork.co.kr).

Heesung Chae is with the ETRI, 161, Gajeong-dong, Yuseong-gu, Daejeon, 305-700, Korea (e-mail: hschae@etri.re.kr).

idea that the pixel for a point at a longer distance has a higher movement speed in the image sequence from the rotating mirror. Like other image-based techniques, this one requires matching points in two images. Since the mirror rotates around an axis that is in parallel with the vertical axis of the image plane, the image near the middle line will basically move horizontally and those away from the middle line will slightly deviate from their corresponding horizontal lines. The image matching error could be reduced because the images are taken by the same camera. The setup provides good flexibility on the view direction. Rotating the mirror is a simple task and will not cause damage or parameter drift to the delicate measurement equipment. Precision improvement is possible and is one attractive merit. It is known that most image-based distance measurement methods cannot provide high precision because of the fact that pixel numbers are integer and thus pixel locations are quantized values. The imprecision caused by the physical limit could be improved through making several measurements and taking an average. With a rotating mirror, more than one pair of images can be taken and the average distance offers a more reliable measurement.

In this paper, the new technique is presented. Precision of the developed measurement scheme and how it is affected have been studied. Experimental results are reported. Section 2 introduces the principle of the proposed monocular vision system. Section 3 presents a practical way for computing the distance. Geometric view is provided for explaining the measurement imprecision for large distance. System calibration is discussed in Section 4. Error analysis with examples illustrating the measurement precision is provided in Section 5. Estimation of image search range for pixel matching for the objects on the non-middle lines has been investigated in Section 6. Experimental results are reported in Section 7 with conclusions given in Section 8.

2. RELATIONSHIP BETWEEN DISTANCE AND PIXEL SPEED

Fig. 1 shows the new distance measurement system. The mirror rotates and reflects images, which are acquired by a camera. It is not hard to perceive the fact that the pixel for a point at a longer distance moves at a faster speed in the sequence of images.

The relationship between the distance and the moving speed of the corresponding pixel can be derived mathematically. Let's first consider the geometry of the image forming on the plane defined by the horizontal middle line of the CCD sensor and the focal point. Let the intersection of the lens axis and the mirror be O, the distance from O to the object T be R as shown in the Fig. 1. Also, let the angle

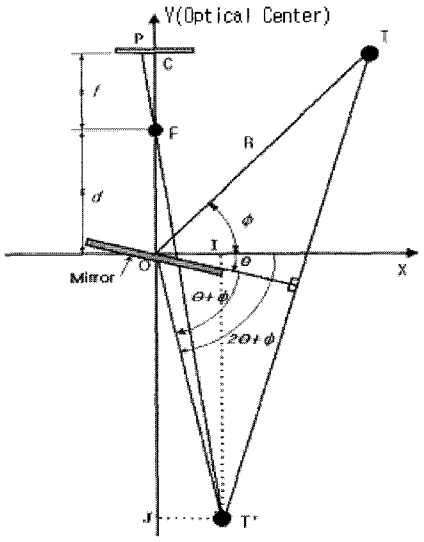

Fig. 1. The distance measurement system with a rotating mirror.

between the line segment OT and the X-axis be ϕ. Then, the position of the object T can be represented in polar coordinates as $R\angle\phi$. Furthermore, let the length from the image plane of the CCD camera to the focal point F be f, the distance from F to O be d, the angle from the X-axis to the mirror be θ (positive in the clockwise direction), and the mirrored location of the object T be T'. Then, the angle between the line segment OT' and the mirror is $\theta+\phi$ and the angle between the line segment OT' and the X-axis becomes $2\theta+\phi$.

Let I and J be the points of projection of T' onto the X-axis and the Y-axis, respectively. Then lengths $\overline{OI}$ and $\overline{OJ}$ can be expressed as

$$\overline{OI} = R\cos(2\theta+\phi), \tag{1}$$

$$\overline{OJ} = R\sin(2\theta+\phi). \tag{2}$$

Let the center of the CCD be C and the image of T' on the CCD be at a point P with the x-coordinate equal to p. From the similarity relationship between ΔFCP and ΔFT'J, the ratio p/f can be obtained as

$$\frac{p}{f} = \frac{-R\cos(2\theta+\phi)}{d+R\sin(2\theta+\phi)}. \tag{3}$$

Note that P is on the left side of the optical center line (vertical line) and thus p has a negative value.

(3) holds even when the object point is not on the X-Y plane. However, for an object point with a non-zero Z-coordinate, the image will be formed either under or above the middle line of the image frame. With the similar geometric derivation, one can easily prove that

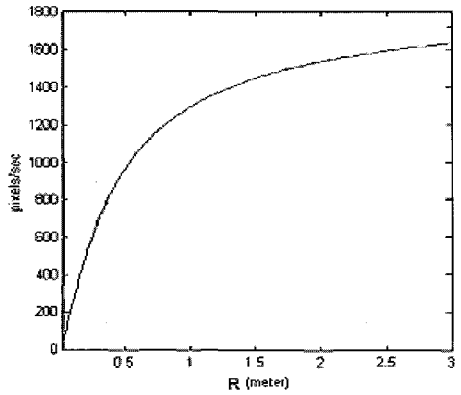

Fig. 2. Pixel speed versus the distance: with $\phi = 70^\circ$, $\theta = 5^\circ$, $f = 6mm$, $d = 200mm$, and $\dot{\theta} = \pi \ rad/\sec$.

$$\frac{z_i}{f} = \frac{-z}{d + R\sin(2\theta + \phi)}, \tag{4}$$

where z is the Z-coordinate of the object point and z_i is the Z-coordinate of the image point on the image plane. Since d and f are constant, and R, ϕ, and z are also constant if the object is not moving, the value z_i, which represents the vertical position of the image point will vary with θ. This will affect the range for image matching search but not the distance computation. The issue will be discussed in a latter section.

Taking the differentiation of (3) with respect to the time and having some mathematical manipulation, one can obtain

$$\dot{p} = 2\frac{(f + \frac{fd}{R}\sin(2\theta+\phi))}{(\frac{d}{R})^2 + 2(\frac{d}{R})\sin(2\theta+\phi) + \sin^2(2\theta+\phi)}\dot{\theta}. \tag{5}$$

The equation shows that the speed of the pixel is a function of several variables including the distance R. Fig. 2 shows the relationship between the pixel speed and the distance to the object when the mirror rotates at the speed of π rad/sec. As shown in the figure, the image of a closer object moves more slowly, and the smaller speed variation for a larger distance (R) indicates that the measurement will become less precise.

3. DISTANCE COMPUTATION FROM TWO IMAGES

3.1. Distance Computation from a Pair of Corresponding Points

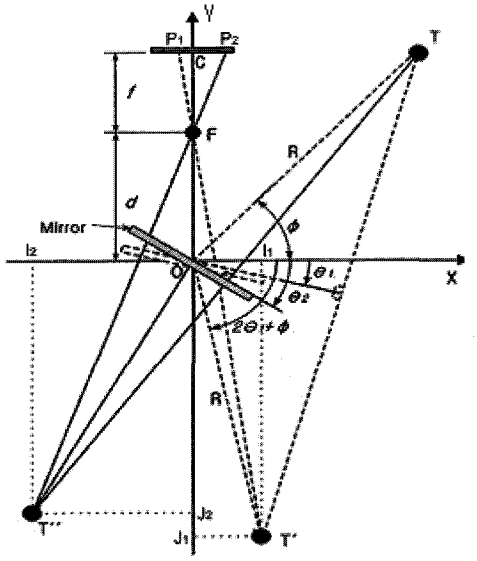

Fig. 3. Distance measurement with tow corresponding pixel position P1 and P2 for mirror angles θ_1 and θ_2.

Distance can be determined from two acquired images Assume that the two images are acquired with the mirror angles at θ_1 and θ_2 (clockwise rotation; see Fig. 3), and the pixel positions are p_1 and p_2, respectively. From (3), one can have the following two equations:

$$\frac{p_1}{f} = \frac{-R\cos(2\theta_1 + \phi)}{d + R\sin(2\theta_1 + \phi)}, \tag{6}$$

$$\frac{p_2}{f} = \frac{-R\cos(2\theta_2 + \phi)}{d + R\sin(2\theta_2 + \phi)}. \tag{7}$$

Note that d and f are constants and the mirror rotation angles θ_1 and θ_2 are known. Pixel locations p_1 and p_2 are determined through the pixel matching processing in the two images. Only R and ϕ are unknown and can be solved from (6) and (7). The distance R can be solved from (6) as

$$R = \frac{-p_1 d}{f\cos(2\theta_1 + \phi) + p_1\sin(2\theta_1 + \phi)} \tag{8}$$

or from (7) as

$$R = \frac{-p_2 d}{f\cos(2\theta_2 + \phi) + p_2\sin(2\theta_2 + \phi)}. \tag{9}$$

Eliminating R in (8) and (9) and expanding cosine and sine terms result in equation (10), which gives equation (11) or equation (12).

$$\begin{aligned}&(p_2 f\cos 2\theta_1 + p_2 p_1 \sin 2\theta_1 - p_1 f\cos 2\theta_2 - p_1 p_2 \sin 2\theta_2)\cos\phi \\ &\quad = (p_2 f\sin 2\theta_1 - p_2 p_1\cos 2\theta_1 - p_1 f\sin 2\theta_2 + p_1 p_2\cos 2\theta_2)\sin\phi\end{aligned} \tag{10}$$

$$\frac{\sin\phi}{\cos\phi} = \frac{fp_2\cos 2\theta_1 + p_1 p_2\sin 2\theta_1 - fp_1\cos 2\theta_2 - p_1 p_2\sin 2\theta_2}{fp_2\sin 2\theta_1 - p_1 p_2\cos 2\theta_1 - fp_1\sin 2\theta_2 + p_1 p_2\cos 2\theta_2} \tag{11}$$

$$\phi = \tan^{-1}\left[\frac{fp_2\cos 2\theta_1 + p_1p_2\sin 2\theta_1 - fp_1\cos 2\theta_2 - p_1p_2\sin 2\theta_2}{fp_2\sin 2\theta_1 - p_1p_2\cos 2\theta_1 - fp_1\sin 2\theta_2 + p_1p_2\cos 2\theta_2}\right] \quad (12)$$

To determine the distance, one may use (12) and (9) or (12) and (5). For the former set, P_1 and P_2 are used and for the latter set the pixel speed must be evaluated.

3.2. Geometric view on how the measurement method works

Fig. 4 can be used to explain geometrically how the proposed measurement method works. As shown in the figure, with the mirror angle equal to θ_1, all the points on the line r_1 are projected onto the same point P_1 (with x-coordinate p_1) on the CCD sensory plane. With the mirror angle changed to θ_2, all points on the line r_2 are projected onto the point P_2 (with x-coordinate p_2). In other words, all the points on r_1 are candidates for having p_1 and all the points on r_2 are candidates for having p_2. If p_1 and p_2 are observed when the mirror angles are θ_1 and θ_2, respectively, the object must reside at the intersection of lines r_1 and r_2. The solution for (9) and (12) is the solution of the two equations representing the lines r_1 and r_2. It is noted that when R increases, the slopes of r_1 and r_2 get closer and the mathematical system with these two equations becomes in ill-condition (two lines are nearly in parallel). Thus, a small error on p_2 could cause a large error on R. Increasing θ_2 - θ_1 will relax the ill-condition and improve the measurement accuracy. However, the overlapped area of two images, *i.e.*, the measurable area, will become smaller. From the figure, one can also see that the effect of inaccurate p_2 on the measurement of the angle ϕ is less significant. A large R introduces only a small error on ϕ. Mathematical analysis on the measurement precision will be done later in Section 5.

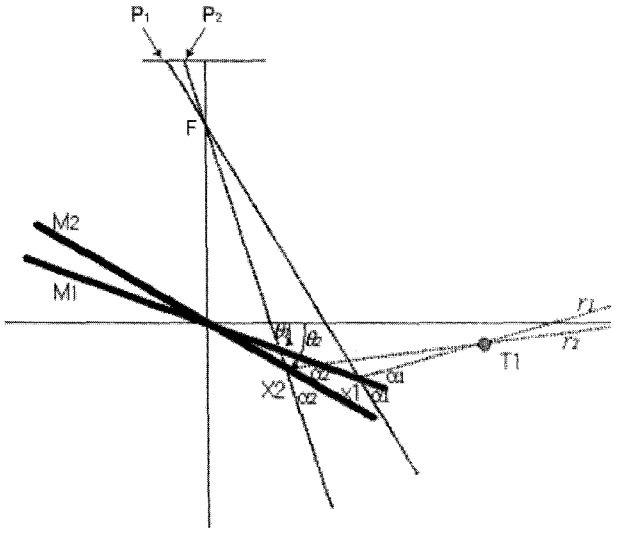

Fig. 4. Geometric view of the measurement.

4. SYSTEM CALIBRATION AND RELAXATION OF THE CORRESPONDENCE PROBLEM

4.1. System calibration

Precise values of the two internal parameters of a CCD camera, the pixel interval and the focal length f, may not be available and need to be calibrated under the real measurement environment. Let the pixel interval be δ. Then, two pixel positions p_1 and p_2 are

$$p_1 = \delta q_1, \quad (13)$$

$$p_2 = \delta q_2, \quad (14)$$

where q_1 and q_2 represent the numbers of pixels from the center of the CCD to the two image points while p_1 and p_2(x-coordinates) give corresponding physical distances. Note that q_1 (or q_2) is a negative integer if the image point is to the left of the CCD center C. Plugging (13) into (8) gives

$$R = \frac{-q_1 d}{\eta\cos(2\theta_1 + \phi) + q_1\sin(2\theta_1 + \phi)}, \quad (15)$$

where η is defined as f/δ, the ratio between the focal length and the pixel interval. The parameter η is the number of pixels equivalent to the length of f. Employing the parameter η, the number of internal parameters of the camera, which needs to be calibrated, is reduced from two to one. The angle ϕ can also be expressed using the parameter η as

$$\phi = \tan^{-1}\left[\frac{\eta q_2\cos 2\theta_1 + q_1q_2\sin 2\theta_1 - \eta q_1\cos 2\theta_2 - q_1q_2\sin 2\theta_2}{\eta q_2\sin 2\theta_1 - q_1q_2\cos 2\theta_1 - \eta q_1\sin 2\theta_2 + q_1q_2\cos 2\theta_2}\right] \quad (16)$$

With a known location (R and ϕ) of an object and its projection points q_1 and q_2, the adequate parameter of η can be determined using (15) and (16).

4.2. Relaxation of the correspondence problem

To calculate the distance using (15) and (16), all pixel matching pairs of (q_1, q_2) should be determined accurately. This is the correspondence problem. If the angle difference between θ_1 and θ_2 is big, images taken at two different angles are very different, which results in that the correspondence problem in the proposed system is also important as in the stereo-vision. In the proposed system, however, two kinds of techniques alleviate such difficulty. Benefits come from the utilization of abundant number of image

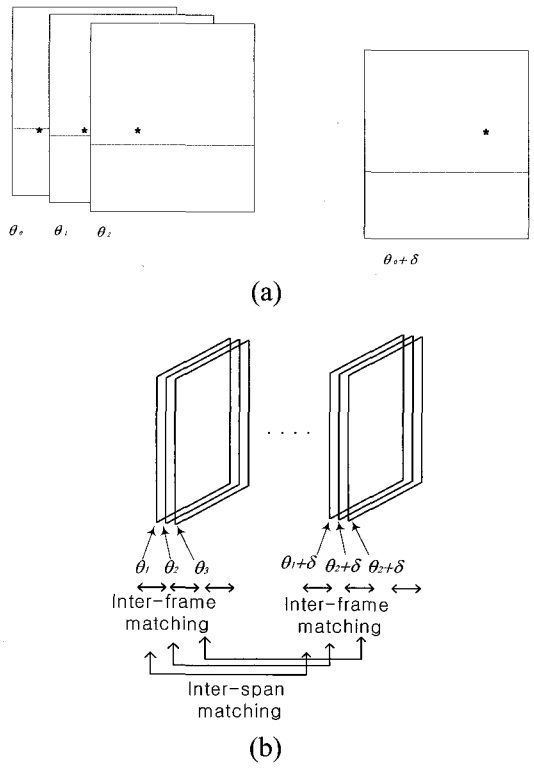

Fig. 5. Relaxation of correspondence problem by (a) tracking of feature points on the image sequence and (b) using multiple pairs of images.

frames. The first technique is with the feature point tracking as in the Fig. 5. In case of matching two images at the angles of θ_0 and $\theta_0 + \delta$, several number of image frames between the two angles are utilized in the proposed system as illustrated in the Fig. 5. Though the matching between two images from big angle difference is difficult, that from small angle difference is easier due to the brightness and the alignment similarities. Matching problem between the bigger angled frames is eased with tracking of the pixels on the closer angled frame. Another technique to relax the correspondence problem is with the utilization of multiple sets of image frames for matching. If the angle between image frames is very small, same scene area can appear commonly on several image frames. Therefore, the matching accuracy can be improved by combining the matching results of several different sets of image frames. For example, the distance of some area can be computed commonly with the multiple image sets of (θ_1, $\theta_1 + \delta$) and of (θ_2, $\theta_2 + \delta$), etc. as in Fig. 5(b). The matching performance can be improved by combining the matching results of such multiple sets of the images.

Above two techniques which are utilizable in the proposed system uniquely enable to relax the correspondence problem.

5. MEASUREMENT ERROR ANALYSIS

The issue of measurement error is addressed in this section.

5.1. Error analysis

Note that q_1 and q_2 are pixel numbers and can only be integers and thus p_1 and p_2 computed from (13) and (14) have quantized values. The quantization causes measurement errors on the direction and distance. To determine a distance, one may try the pixel matching to find p_2 (from pixel q_2) in the second image that is corresponding to the image point at p_1 (from pixel q_1) in the first image. With the image at p_1 as a reference pixel, no error on p_1 needs to be considered. However, theoretically, there could be an error of up to $\pm$ 0.5 pixels on q_2 due to the quantization. It is possible that the practical pixel mismatching error is larger. How sensitive the measured distance and direction are to a pixel mismatching error will be evaluated as the *distance error sensitivity* and the *direction error sensitivity*.

The measurement error sensitivities are examined below. The distance error sensitivity can be evaluated by taking the derivative of R with respect to p_2 as

$$\frac{dR}{dp_2} = \frac{dR}{d\phi}\frac{d\phi}{dp_2}. \tag{17}$$

With (8), $dR/d\phi$ can be expressed as

$$\frac{dR}{d\phi} = \frac{(-fp_1 d\sin(2\theta_1+\phi) + p_1^2 d\cos(2\theta_1+\phi))}{(f\cos(2\theta_1+\phi) + p_1\sin(2\theta_1+\phi))^2}. \tag{18}$$

For convenience, let the numerator and denominator of the right side of (11) be ω and ψ, respectively, *i.e.*,

$$\tan\phi = \frac{\sin\phi}{\cos\phi} = \frac{\omega}{\psi}, \tag{19}$$

where

$$\omega = fp_2\cos 2\theta_1 + p_1p_2\sin 2\theta_1 - fp_1\cos 2\theta_2 - p_1p_2\sin 2\theta_2 \tag{20}$$

and

$$\psi = p_2\sin 2\theta_1 - p_1p_2\cos 2\theta_1 - fp_1\sin 2\theta_2 + p_1p_2\cos 2\theta_2. \tag{21}$$

Differentiating (19) with ϕ and p_2 as variables gives

$$\frac{1}{\cos^2\phi}d\phi = \frac{\psi\frac{d\omega}{dp_2} - \omega\frac{d\psi}{dp_2}}{\psi^2}dp_2, \tag{22}$$

where

$$d\omega = (f\cos 2\theta_1 + p_1\sin 2\theta_1 - p_1\sin 2\theta_2)dp_2, \tag{23}$$

and

$$d\psi = (f\sin 2\theta_1 - p_1\cos 2\theta_1 + p_1\cos 2\theta_2)dp_2. \tag{24}$$

$$\frac{d\phi}{dp_2} = \frac{f^2 p_1 \sin(2\theta_1 - 2\theta_2) - fp_1^2 \cos(2\theta_1 - 2\theta_2) + fp_1^2}{(p_2^2 + f^2)p_1^2 + (p_1^2 + f^2)p_2^2 - 2fp_1p_2(p_1 - p_2)\sin(2\theta_1 - 2\theta_2) - 2p_1p_2(f^2 + p_1p_2)\cos(2\theta_1 - 2\theta_2)}. \quad (25)$$

$$\frac{dR}{dp_2} = \frac{(-fp_1 d\sin(2\theta_1 + \phi) + p_1^2 d\cos(2\theta_1 + \phi))}{(f\cos(2\theta_1 + \phi) + p_1\sin(2\theta_1 + \phi))^2} \cdot \frac{f^2 p_1 \sin(2\theta_1 - 2\theta_2) - fp_1^2 \cos(2\theta_1 - 2\theta_2) + fp_1^2}{(p_2^2 + f^2)p_1^2 + (p_1^2 + f^2)p_2^2 - 2fp_1p_2(p_1 - p_2)\sin(2\theta_1 - 2\theta_2) - 2p_1p_2(f^2 + p_1p_2)\cos(2\theta_1 - 2\theta_2)}$$
$$= R^2 \cdot \frac{(f\sin(2\theta_1 + \phi) - p_1\cos(2\theta_1 + \phi))}{d} \cdot \frac{-f^2\sin(2\theta_1 - 2\theta_2) + fp_1\cos(2\theta_1 - 2\theta_2) - fp_1}{(p_2^2 + f^2)p_1^2 + (p_1^2 + f^2)p_2^2 - 2fp_1p_2(p_1 - p_2)\sin(2\theta_1 - 2\theta_2) - 2p_1p_2(f^2 + p_1p_2)\cos(2\theta_1 - 2\theta_2)}. \quad (26)$$

Plugging (20), (21), (23), and (24) into (22), and using $1 + \tan^2\phi = 1/\cos^2\phi$ and (19), one can obtain (25). (25) is the direction error sensitivity. Only p_2 is the variable in (25). Plugging (18) and (25) into (17), the sensitivity of R on p_2 becomes (26).

The sensitivity, dR/dp_2, is proportional to R^2. The measurement becomes less accurate at a longer distance. It is also noted that the sensitivity is inversely proportional to d. Thus the measurement precision should be better with a larger d.

5.2. An insight into the measurement error

It is not easy to see clearly from the derived equations how factors affect the error sensitivity and the measurement error. Fig. 6 shows some error sensitivity plots for the case with $\theta_1 = 0^\circ$, $\theta_2 = 12^\circ$, $R \in [1,10]$m and $\phi \in [70^\circ, 85^\circ]$. The values of f and d are (6mm, 200mm), (6mm, 100mm) and (12mm, 200mm) for three sets of plots of dR/dp_2 and $d\phi/dp_2$. The following are observed from (26) and Fig. 6:

1) If $\sin(2\theta_1 - 2\theta_2)$ is not much smaller than $\cos(2\theta_1 - 2\theta_2)$ and $p_1 << f$ and $p_2 << f$, the distance error sensitivity in (26) can be simplified to

$$\frac{dR}{dp_2} \cong \frac{-R^2 \quad f\sin(2\theta_1 + \phi)\sin(2\theta_1 - 2\theta_2)}{d(p_1^2 + p_2^2 - 2p_1p_2\cos(2\theta_1 - 2\theta_2))}. \quad (27)$$

Since p_i's are approximately proportional to f as seen in (5), dR/dp_2 in the above equation will be inversely proportional to the focal length f. From Figs. 6(a1) and 6(a2), one can see that the sensitivity dR/dp_2 is reduced to about one half if the focal length is doubled. Note that the focal length is 6mm and P_1 and P_2 are in [-2.2mm, 2.2mm]. (26) and (27) also show that the distance error sensitivity is proportional to R^2.This can be seen in each of Figs. 6(a1), 6(a2) and 6(a3). The sensitivity should be inversely proportional to d as observed in Figs. 6(a1) and 6(a3). Note that they use different scale for the vertical axis.

2) The direction error sensitivity in (25) can be simplified to

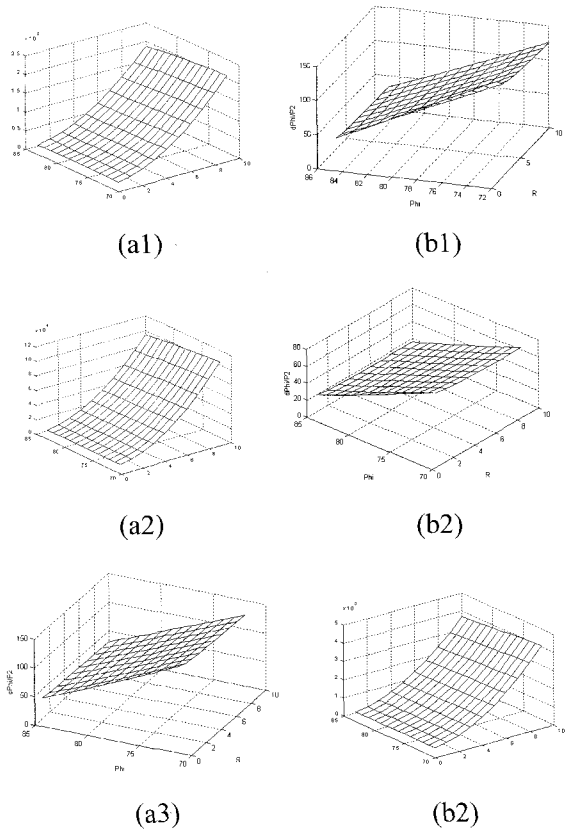

(a1) (b1)

(a2) (b2)

(a3) (b2)

Fig. 6. Plots for sensitivities dR/dp_2 and $d\phi/dp_2$ with different f and d. Angles θ_1 and θ_2 are selected to be 0° and 12°.

(a1) dR/dp_2 with f=6mm, d=200mm

(b1) $d\phi/dp_2$ with f=6mm, d=200mm,

(a2) dR/dp_2 with f=12mm, d=200mm

(b2) $d\phi/dp_2$ with f=12mm, d=200mm

(a3) dR/dp_2 with f=6mm, d=100mm

(b3) $d\phi/dp_2$ with f=6mm, d=100mm

$$\frac{d\phi}{dp_2} \cong \frac{p_1 \sin(2\theta_1 - \theta_2)}{(p_1^2 + p_2^2 - 2p_1 p_2 \cos(2\theta_1 - \theta_2))} \quad (28)$$

Since p_i's are approximately proportional to f, the direction error sensitivity will be inversely proportional to the focal length f. However, the sensitivity is not affected directly by R and d. From Figs. 6(b1) and 6(b2), one can see that the sensitivity $d\phi / dp_2$ is reduced to about one half if the focal length is doubled. From Fig. 6(b1) and 6(b3), one observes that the sensitivity $d\phi / dp_2$ keeps almost constant even though the distance d is doubled.

3) One can estimate the measurement error on distance for one-half pixel error. If the width of the CCD sensor is 4.4mm and there are 320 pixels, then the horizontal distance between two adjacent pixels is 0.0138mm. For the results for Fig. 6(a1), the sensitivity at $R \cong$ 6m and $\phi = 75^o$ is $0.7528*10^5$. The estimated measurement error from one-half pixel position error will be $0.5*(0.7528*10^5)*(0.0138*10^{-3}) = 0.52$m. This will be reduced to 0.26m if a camera with two times the focal length is used.

4) One can also estimate the measurement error for the angle ϕ for one-half pixel error. From Fig. 6(b1), the sensitivity at R = 6m and $\phi = 75^o$ is 104.9. The estimated measurement error will then be $0.5*(104.9)*(0.0138*10^{-3}) = 7.2*10^{-4}$ radium, which is a negligible amount.

6. SIMULATION AND EXPERIMENTS

6.1. Simulation results

Since the proposed distance measurement system is based on the pixel matching between two image frames which appear on a mono-camera, the major cause of the error is from the pixel mismatching. In this simulation study, the distance measurement error caused from one pixel mismatching is estimated for several different conditions. The plots in Fig. 7 show what the errors on the angle and the range will be given a unit error on q_2,. The mirror rotation angle is selected to be $\theta_1 - \theta_2 = 14^0$ and 6^0. For each pair of given (q_1, q_2) and (q_1, q_2+1), the angles and ranges are calculated. These two points are plotted in the figure with a line segment connecting them. Thus, a longer line indicates a larger possible error. In Fig. 7(a), the values of q_1 are in [–80, 85] with an interval of 15 (*i.e.*, -80, -65, -50, ... 70, 85). The values of q_2 also start from –80 with an interval of 5 (*i.e.*, -80, -75, -70, ... 180). In Fig. 7(b), the ranges of q_1 and q_2 are [-110, 115] and [-10, 50], respectively, with the same incremental sizes 15 and 5. It is seen that the line segments get longer at farther distances; *i.e.*, the measurement accuracy is worse at a longer distance. However, the error on the direction is insignificant. The shorter segments in Fig. 7(a), compared to those in Fig. 7(b), indicate that a larger $|\theta_2 - \theta_1|$ provides a better measurement accuracy.

The above results are for objects in the direction near the Z-axis (i.e., $\phi \approx 90^o$). The measurable direction can be altered by changing the mirror facing direction. Fig. 8 shows the similar results for the cases with ϕ close to 180^o, 90^o and 0^o. It is seen that the errors are all similar regardless of the measuring direction.

6.2. Experiments

The real distance measurement system has been tested. The image size is 320 (H)×240 (V) and the parameter $\eta = \frac{f}{\delta}$ is 440. The size of the plane mirror is 110 mm× 60 mm and its distance to the camera, d is 200 mm. Fig. 9 shows two images, which were taken through the mirror before and after a 5^o rotation in the clockwise direction. One can see that

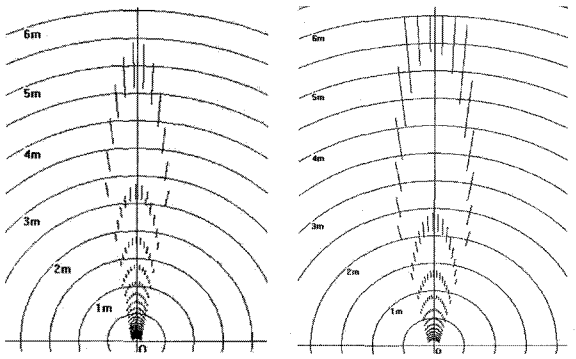

(a) $\theta_1 - \theta_2 = 14^0$ (b) $\theta_1 - \theta_2 = 6^0$

Fig. 7. Distance and direction errors caused by 1 pixel mismatching.

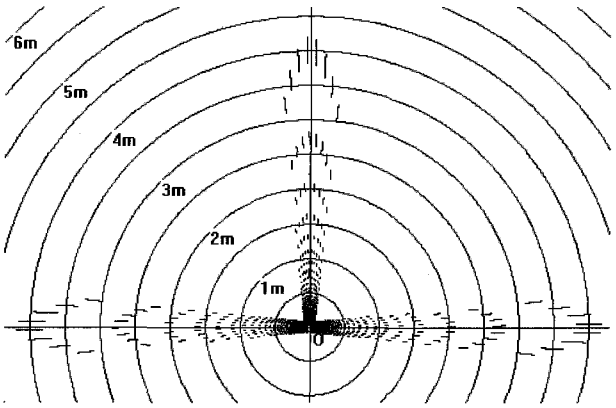

Fig. 8. Distance measurement error for 1 pixel mismatching at different measurement directions. Error ranges at the left, center, and right groups are obtained with the mirror angles from -38^o to -52^o, 7^o to -7^o, and from 52^o to 38^o, respectively.

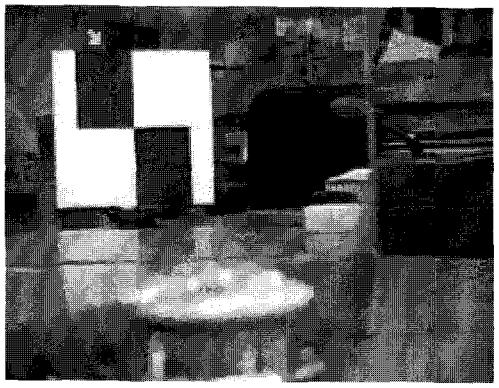

(a)

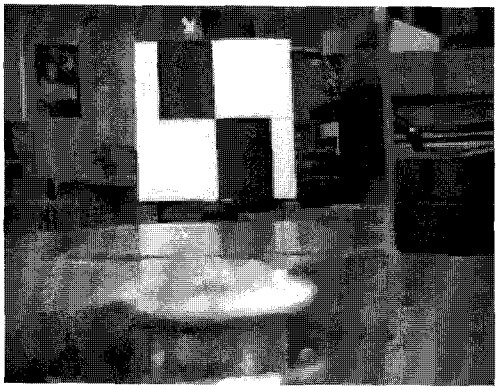

(b)

Fig. 9. A pair of images acquired through the rotating mirror (a) before rotation, (b) after rotation.

the relative positions between the vertical central line of the white board and the dark background object pointed by an arrow are different in two images. The line on the board moves less than that of the background object in the images because its distance is smaller.

The measured distances are compared to the real distances in Fig. 10. The measured object is located along the line with $\phi = 80^{o}$ but has the distance varied.

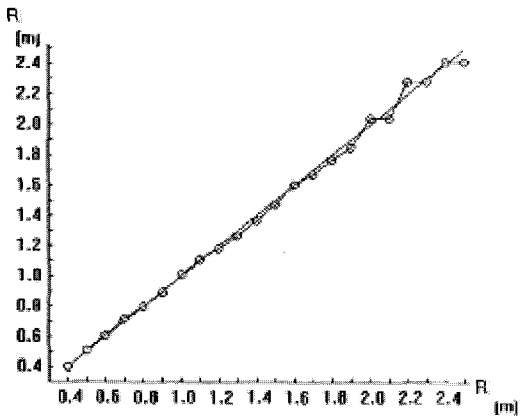

Fig. 10. Distance measurement error. The straight line corresponds to zero error and the zigzag curve with circle marks indicates the real measurement.

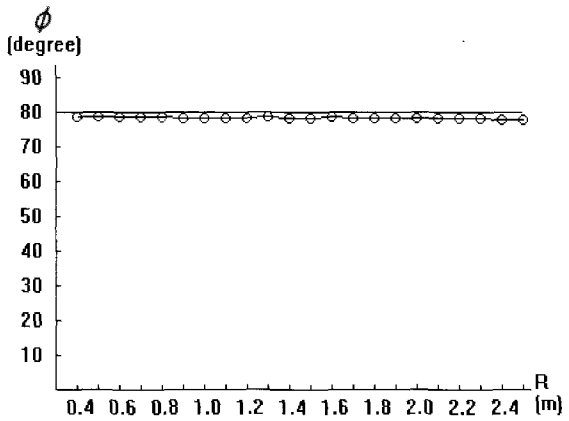

Fig. 11. Direction measurement error. The straight line indicates the real angle and the circle marks indicate the measured angles.

The straight line in the figure represents the actual distance for points on the line with $\phi = 80^{o}$ and the zigzag curve with small circles shows the measured distances using the proposed system. One can see that the errors seem to be random either positive or negative. This suggests that taking an average of several measurements for the same object during the mirror's rotation should improve accuracy. The results in the figure show that the error is negligible within the distance of 2m. The error increases with the distance and is about 10 cm at the distance of 2.5m. Fig. 11 shows the corresponding direction errors, which remain small.

7. CONCLUSIONS

The proposed distance measurement system has a camera installed in front of a rotary plane mirror. With the mirror rotating, the pixel for an object point at a longer distance will move faster in the image. Using two images taken with the mirror at different angles, the different pixel positions for the same object point can be used to compute the distance. Equations needed to compute the distance have been derived and presented. Precision improvement is possible and is one attractive merit of the new technique. Our experiments show that the measurement errors are, randomly, positive or negative. This suggests that the imprecision caused by the physical limit could be improved through making several measurements and taking an average. The presented approach with a rotating mirror is especially suitable for such multiple measurements. With a rotating mirror, more than one pair of images can be easily taken and the average distance will offer a more reliable measurement result. Other attractive characteristics of the new measurement system include the simpler hardware, the easiness of pixel matching, no camera movement and the flexibility of measurement view direction.

REFERENCES

[1] M. El Ansari, L. Masmoudi, and L. Radouane, "A new region matching method for stereoscopic images," *Pattern Recognition Letters*, vol. 21, pp. 283-294, April 2000.

[2] W. E. L. Grimson, "Computational experiments with a feature based stereo algorithm," *IEEE Trans. on Pattern Analysis and Machine Intelligence*, vol. PAMI-7, no. 1, pp. 17-33, January 1985.

[3] F. Candocia and M. Adjouadi, "A similarity measurement for stereo feature matching," *IEEE Trans. on Image processing*, vol. 5, pp. 1460-1464, October 1997.

[4] W. Choi, C. Ryu, and H. Kim, "Navigation of mobile robot using mono-visio and mono-audition," *IEEE Computer*, vol. 22, no. 6, pp. 46-57, 1989.

[5] H. Zhuang, R. Sudhakar, and J. Shieh, "Distance estimation from a sequence of monocular images with known camera motion," *Robotics and Autonomous Systems*, vol. 13, pp. 87-95, 1994.

[6] G. Sandini and M. Tistarelli, "Active tracking strategy for monocular distance inference over multiple frames," *IEEE Trans. on Pattern Analysis and Machine Intelligence*, vol. 12, no. 1, pp. 13-27, January 1990.

[7] C. E. Smith, S. A. Brandt, and N. P. Papanikolopoulos, "Eye-in-hand robotic tasks in uncalibrated environments," *IEEE Trans. on Robotics and Automation*, vol. 13, no. 6, pp. 904-1014, December 1997.

[8] J. T. Feddema, and C. S. G. Lee, "Adaptive image feature prediction and control for visual tracking with a hand-eye-coordinated camera," *IEEE Trans. on Systems, Man, and Cybernetics*, vol. 20, no. 5, pp.1172-1183, September/ October 1990.

[9] A. Goshtasby and W. Gruver, "Design of a single-lens stereo camera system," *Pattern Recognition*, vol. 26, no. 6, pp. 923-937, 1993.

[10] U. R. Dhond and J. K. Aggarwal, "Structure from stero- a review," *IEEE Trans. on System, Man and Cybernetics*, vol. 19, pp. 1489-1510, November/December 1989.

[11] P. Puget and T. Skordas, "An optimal solution for mobile camera calibration," *IEEE Trans. on System, Man and Cybernetics,* vol. 19, no. 6, pp. 1426-1445, November/December 1988.

[12] Z. Zhang and O. D. Faugeras, "Calibration of a mobile robot with application to visual navigation," *Proc. IEEE Work. Visual Motion*, Irvin, California, pp. 306-313, March 1989.

[13] M. Inaba, T. Hara, and H. Inoue, "A stereo viewer based on a single camera with view-control mechanism," *Proc. of the International Conference on Robots and Systems*, vol. 3, pp. 1857-1865, July 1993.

[14] S. K. Nayar, "Sphereo: Determining distance using a single camera and two specular spheres," *Proc. of SPIE: Optics, Illumination, and Image Sensing for Machine Vision* II, pp. 245-254. November 1988.

[15] S. Nene and S. Nayar, "Stereo with mirrors," *Proc. of the 6th International Conference on Computer Vision*, pp. 1087-1094, January 1998.

[16] N. P. Papanikolopoulos, P. K. Khosla, and T. Kanade, "Visual tracking of a moving target by a camera mounted on a robot; A combination of control and vision," *IEEE Trans. on Robotics and Automation*, vol. 9, no. 1, pp. 14-35, February 1993.

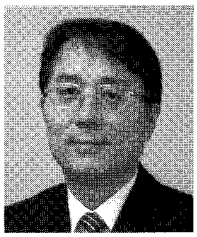

Hyongsuk Kim received the B.S degree in Electronics Engineering from the Hanyang University, Republic of Korea in 1980. He received the M.S in Electrical Engineering from the Chonbuk National University, Republic of Korea in 1982. He received the Ph.D. degree in Electrical Engineering from the University of Missouri, Columbia, in 1992. During the period of 1982-1993, he worked for the Agency for Defense Development, Republic of Korea. Since 1993, he has been a Professor with the Division of Electronics and Information Engineering, Chonbuk National University, Republic of Korea. From 2000 to 2002, he was with the Nonlinear Electronics Laboratory, EECS Department, University of California, Berkeley, as a Visiting Scholar. His current research interests include Cellular Neural/Nonlinear Networks and its application to image processing and communication problems.

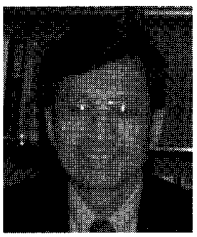

Chun-Shin Lin received the Ph.D. from School of Electrical Engineering at Purdue University in 1980.He worked as an Associate Research Fellow at Academia Sinica from 1981-1984. He was on faculty of Electrical and Computer Engineering Department at San Diego State University from 1984-1987 and has been with the University of Missouri-Columbia since 1987. He spent many summers doing research at research labs including JPL, NASA Lewis Research Center, Langley Research Center and Johnson Space Center, US Air Force Wright Patterson Lab and Eglin Research Lab as well as US Naval Research Center. Dr. Lin was a Technical Editor for the IEEE Transactions on Robotics and Automation from 1991-1993. In 2003-2004, he made a six-month visit at Chonbuk National University in Korea and a six-month visit at Air Force Research Lab at Rome, NY. His past research covered robotics and neural networks funded by two NSF grants and several contracts from US Air Force.His current interest is on high performance computation with a focus on reconfigurable computation.

Jaehong Song received the B.E. degree in Control and Instrumentation Engineering from Chonbuk National University, Republic of Korea in 1999. He received the M.E. in Control and Instrumentation Engineering from Chonuk National University, Republic of Korea in 2002. From 2002 to 2004, he worked as a control and monitoring system developer for Bluecord Techonology Co., Ltd. Republic of Korea. Since 2004, he has been a controller developer for Syswork Co., Ltd. Repulic of Korea.

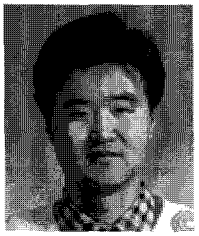

Heesung Chae received the B.S. and M.S. degree in Control and Instrumentation Engineering from Chonbuk National University, Korea in 1998 and 2000. He has been a staff of the Electronics and Telecommunications Research Institute (ETRI) since 2000. He is now engaged in the project of the ubiquitous robot supported by Ministry of Information and Communication, Korea. His current research interests include Localization/Navigation of mobile robot.